TMEM225: A possible protein phosphatase 1 γ 2 (PP1 γ 2) regulator localizes to the equatorial segment in mouse spermatozoa

TMEM225: a possible PP1γ2 regulator localizing to the equatorial segment in mouse spermatozoa

Short title: TMEM225 is a possible regulator of PP1γ2

Minami Matsuura and Keiichiro Yogo*

Laboratory of Animal Physiology, Graduate School of Agriculture, Shizuoka University, Shizuoka 422-8529, Japan

*Correspondence to: Keiichiro Yogo, Laboratory of Animal Physiology, Graduate School of Agriculture, Shizuoka University, 836 Ohya, Suruga, Shizuoka 422-8529, Japan

Tel/Fax: 81-54-238-4868; E-mail: yogo.keiichiro@shizuoka.ac.jp

Keywords: spermatogenesis, acrosome, protein phosphatase, spermatid, membrane protein

Abbreviations: PP1, protein phosphatase 1; IP-western, immunoprecipitation-western blotting; RT-PCR, reverse transcription-polymerase chain reaction; GST, glutathione S-transferase; PKA, protein kinase A; SDS-PAGE, sodium dodecyl sulfate polyacrylamide gel electrophoresis; IPTG, isopropyl β-D-1-thiogalactopyranoside; PBS, phosphate buffered saline; DAPI, 4,6-diamidino-2-phenylindole: DTT, dithiothreitol; PNA, peanut agglutinin.

Grant sponsor: United Graduate School of Agricultural Science (Gifu University) Education and Research Activation Grants

Abstract

We previously identified *Tmem225* as one of 53 spermatogenesis-associated transmembrane protein genes. *Tmem225* encodes a putative four-transmembrane domain protein that has an RVxF motif known to be a consensus site for interaction with serine/threonine protein phosphatase 1 (PP1); however, the physiological function of TMEM225 has not been elucidated. In this study, we investigated the expression and molecular characteristics of TMEM225 in mice. *Tmem225* and its expression product were found to be specific to germ cells in the testes, with expression increasing during spermatogenesis. In mature spermatozoa, TMEM225 is localized to the equatorial segment of the acrosome but not to the midpiece or tail. TMEM225 appears to be an outer and/or inner acrosomal membrane protein, and the TMEM225 in the dorsal region of the acrosome seemed to be lost after acrosome reaction. TMEM225 interacts with PP1 *in vivo*, and a pull-down assay revealed that the C-terminal region of TMEM225 could bind to PP1γ2, a predominant isoform of PP1 in male germ cells. In addition, TMEM225 inhibited PP1γ2 activity *in vitro*, and the RVxF motif was essential for inhibition. Since activity of PP1γ2 is necessary for normal spermatogenesis and relevant to capacitation and motility in spermatozoa, our results suggest that TMEM225 is involved in the differentiation and function of spermatozoa through the regulation of PP1γ2 activity in mice.

Introduction

Mammalian spermatogenesis is a complex process that involves mitotic proliferation, meiotic division, and postmeiotic differentiation. In the late phase of spermatogenesis, spermatids undergo dynamic morphological and biochemical changes required for fertilization (Clermont 1972; Eddy 1998), and a large number of germ cell-specific genes begin to be expressed in haploid spermatids (Schultz et al. 2003; Shima et al. 2004), and these are thought to play a critical role in the differentiation and function of germ cells. However, the molecular functions of most genes remained to be elucidated.

Membrane proteins constitute about 30% of all proteins and play fundamental roles in cellular functions such as signal transduction, ion transport, cell-cell interactions, and intracellular membrane trafficking. Because of their biological significance, membrane proteins are considered promising targets for drug discovery. In fact, almost half of the drugs currently on the market target membrane proteins (Cooper 2002). In mammalian spermatozoa, several membrane proteins that are essential for fertility have been found. For example, Izumo, an immunoglobulin domain-containing type I membrane protein, is necessary for membrane fusion of eggs in mice (Inoue et al. 2005). In addition, *Catsper1*, a voltage-gated Ca^{2+} channel, is required in flagellar motility for hyperactivation and fertilization in mice (Carlson et al. 2003). However, a comprehensive search for membrane proteins expressed in spermatozoa has not been performed.

To understand the molecular mechanisms of differentiation and function of mammalian spermatozoa and to find a potential target for fertility drugs, we previously screened for spermatogenesis-associated transmembrane protein genes in mice using an *in silico* approach (Yogo et al. 2012). Fifty-three genes were identified including *Tmem225* (also known as *Pmp20cd*). *Tmem225* is conserved in rat, dog, cow, chimpanzee, and human genomes and encodes a protein predicted to have 4 transmembrane helices. In addition, TMEM225 contains a conserved C-terminal RVxF motif, which is a known consensus sequence for interaction with protein phosphatase 1 (PP1). Recently, human TMEM225 was identified as a protein phosphatase 1 (PP1) α-interactor using an *in silico* approach (Hendrickx et al. 2009). However, the physiological function of *Tmem225* remains to be elucidated.

Protein phosphorylation and dephosphorylation play an important role in the regulation of many cellular processes including cell proliferation and differentiation. PP1, a major serine/threonine protein phosphatase in eukaryotes, has 3 catalytic subunit isoforms, PP1α, PP1β, and PP1γ, and PP1γ has 2 variants (PP1γ1 and PP1γ2) made by alternative splicing of the *Ppp1cc* gene. Among these PP1 isoforms, PP1γ2 is predominant in the testes and is expressed in secondary spermatocytes, spermatids, and epididymal

spermatozoa (Chun et al. 1994; Chakrabarti et al. 2007). PP1γ2 is localized throughout spermatozoa but concentrates in the anterior acrosome and in the equatorial segment (Huang et al. 2002). Deficiencies of the *Ppp1cc* gene cause male infertility in mice due to impaired spermatogenesis (Varmuza et al. 1999; Chakrabarti et al. 2007), indicating that PP1γ2 plays an indispensable role in this process. In addition, protein phosphatase activity also affects capacitation and motility of spermatozoa. For instance, treatment with a phosphatase inhibitor such as okadaic acid enhanced sperm motility in cow and human subjects (Smith et al. 1996; Vijayaraghavan et al. 1996). Since the activity and substrate specificity of the PP1 catalytic subunit are defined by various regulatory proteins expressed in a spatially and temporally-specific manner (Cohen and Cohen 1989), we hypothesized that TMEM225 is one such regulator in male germ cells. Recently, Yang et al. reported that *Tmem225* mRNA is specifically expressed in the rat testis over 13 months of age and that the expression is detected in spermatocytes and round-spermatids (Yang et al. 2011). However, the protein expression profile in testes has not been investigated, and whether TMEM225 can act as a PP1γ2 regulator remains to be elucidated. In this study, we investigated the expression, intracellular localization, and biochemical characteristics of TMEM225 in mice.

Results

Tissue distribution and postnatal testicular expression of Tmem225

We first examined the expression of *Tmem225* mRNA in various mouse tissues using reverse transcription-polymerase chain reaction (RT-PCR) and found that *Tmem225* is predominantly expressed in the testis (Fig. 1A). Expression was not observed in W/W^{v} mouse testes, which are known to lack germ cells (Fig. 1B), indicating that *Tmem225* is specifically expressed in germ cells. We next investigated the expression of *Tmem225* in testes during postnatal development and found that it began 25 days after birth and continued thereafter (Fig. 1C). Since the first spermatids appear around 20 days after birth (Bellve et al. 1977), these results suggest that *Tmem225* expression begins in developing spermatids.

Expression and testicular distribution of TMEM225

To investigate the protein expression profile of TMEM225, we developed an anti-TMEM225 antibody and confirmed its specificity by immunoprecipitation followed by western-blotting (IP-western) using overexpressed FLAG-tagged TMEM225 (Fig. 2A). We then examined the tissue specificity and postnatal developmental expression of TMEM225 using IP-western (Fig. 2B and 2C). The tissue specificity of

TMEM225 expression was similar to that of its mRNA, whereas postnatal testicular expression of TMEM225 appeared to be slightly delayed compared to mRNA expression, suggesting that TMEM225 expression is regulated at not only the transcriptional level but also at the translational level. In addition, we found that TMEM225 expression could be detected in epididymides and isolated epididymal spermatozoa.

These results were confirmed by immunohistochemical analysis of the testes and epididymides. TMEM225 signals were observed in germ cells but not in somatic cells such as Leydig cells and epithelial cells of the epididymis (Fig. 3A and 3B). Further, we determined the stages of spermatogenesis during which TMEM225 is expressed as previously described (Yogo et al. 2012) and found that TMEM225 is expressed in spermatids of the maturation phase (steps 15–16) at stages IV–VIII (Fig. 3B).

Intracellular localization of TMEM225

To investigate the intracellular localization of TMEM225 in mature spermatozoa, epididymal spermatozoa were smeared on glass slides and stained with anti-TMEM225 antibody. TMEM225 was found in the head but not in the midpiece or tail (Fig. 4A, left panel). When viewed at higher magnification, TMEM225 appeared to be localized specifically to the acrosome and not to the post-acrosomal region (Fig. 4A, right panel). When the antibody was absorbed with excess glutathione S-transferase (GST)-TMEM225 fusion protein containing the antigen region, the signals completely disappeared (Fig. 4B). Moreover, another TMEM225 antibody (#64) also stained the same region of the head (Fig. 4B), suggesting that these signals are specific for TMEM225. The acrosomal region consists of two different regions: the anterior acrosome and the posterior acrosome (also known as the equatorial segment). We investigated TMEM225 localization in more detail using double immunofluorescence staining with sp56, a marker for the anterior region of the acrosome (Cohen and Wassarman 2001; Kim et al. 2001). TMEM225 did not colocalize with sp56 (Fig. 4C), suggesting that TMEM225 predominantly localizes to the equatorial segment of mouse spermatozoa. Accordingly, confocal microscopic analysis of a vertical section of epididymal spermatozoa revealed that TMEM225 is localized to both sides of the head, presumably in the equatorial segment, but not in the apical region of head (Fig. 4D).

Sperm heads are covered by three membranes: the plasma membrane, the outer acrosomal membrane, and the inner acrosomal membrane. To investigate whether TMEM225 is a plasma membrane protein, we examined the sensitivity of proteinase K digestion for TMEM225 and found that TMEM225 in intact spermatozoa was not digested by proteinase K, whereas TMEM225 in the solubilized lysate was digested (Fig.

5). These results suggest that most or all of TMEM225 does not localize to the plasma membrane and may localize to the outer and/or inner acrosomal membrane.

Effects of capacitation and acrosome reaction on intracellular localization

Next, we examined the effect of capacitation and acrosome reaction on intracellular localization of TMEM225. Although a marked change of TMEM225 localization was not observed after capacitation, immunostaining signals slightly decreased after acrosome reaction in spermatozoa, especially in the dorsal region of the acrosome (Fig. 6A, arrowhead). Similar changes were observed for both a calcium ionophore, A23187, and progesterone, a natural inducer of the acrosome reaction. In fact, quantification by image analysis revealed that the stained area decreased by about 30% after the acrosome reaction (Fig. 6B). These results suggest that a portion of TMEM225 is lost with the acrosome reaction.

TMEM255 binds and inhibits PP1γ2

Finally, we investigated whether TMEM225 can act as a regulator of PP1γ2. Using IP-western analysis, we found that TMEM225 interacts with PP1 *in vivo* (Fig. 7A). Since the anti-PP1 antibody recognizes all PP1 isoforms, we further examined its interaction with PP1γ2 using a pull-down assay and found that the C-terminal region of TMEM225 (TMEM225C-wt) could bind to PP1γ2, but TMEM225C-mt, a deletion mutant lacking the RVxF motif, could not bind (Fig. 7B). Many RVxF motif-containing PP1 interactors act as inhibitors; therefore, we investigated the ability of TMEM225 to inhibit PP1γ2 activity *in vitro*. As expected, TMEM225C-wt inhibited the phosphatase activity in a dose-dependent manner, whereas TMEM225C-mt did not show a significant inhibitory effect (Fig. 7C).

Discussion

The expression profile of *Tmem225* was first reported in rat by Yang et al. (Yang et al. 2011), who found that rat *Tmem225* is specifically expressed in the testis, where it is expressed mainly in spermatocytes and round spermatids. They also found that *Tmem225* is expressed only after 13 months and concluded that *Tmem225* is an age-related gene that may not play a role in the first wave of spermatogenesis. In this study, we demonstrated that *Tmem225* expression starts at day 25 after birth, during the first wave of spermatogenesis in mouse testes, and that it is restricted to elongated spermatids and mature spermatozoa. This expression pattern is apparently different from that of rat *Tmem225*. The precise reason for this discrepancy is not clear; however,

our results are consistent with the expression profile from DNA microarray analysis during mouse spermatogenesis, which is reported by two independent laboratories (Schultz et al. 2003; Shima et al. 2004). Furthermore, we investigated the protein expression profile and found that it was essentially the same as that for the mRNA. These results strongly suggest that *Tmem225* is expressed in mice during the first wave of spermatogenesis and that its expression is specific to postmeiotic germ cells.

One major finding of this study is that TMEM225 is predominantly localized to the equatorial segment in mature spermatozoa. The equatorial segment first becomes apparent during late spermatogenesis, when the round spermatid is transformed into an elongated spermatozoon (Jones et al. 2008). Freeze-fracture electron microscopy (Phillips 1977) and atomic force microscopy (Allen et al. 1995; Ellis et al. 2002) revealed that the equatorial segment has structural features distinct from other regions of the head. In concurrence with this, a variety of proteins such as equatorin (Toshimori et al. 1998), SAMP32 (Hao et al. 2002), and SPESP1 (Wolkowicz et al. 2003) exhibit localization restricted to the equatorial segment. Although the equatorial segment is present in all eutherians, it has not been identified in marsupial, monotreme, or chicken spermatozoa (Bedford et al. 1979). Interestingly, the *Tmem225* gene was found only in the eutherian genome but not in other mammalian (metatherian and prototherian) or vertebrate genomes by gene search using a public database (http://www.ncbi.nlm.nih.gov/gene/). The only exception is the gray short-tailed opossum (marsupial); however, the deduced amino acid sequence of TMEM225 lacks the conserved RVxF motif. These results suggest that TMEM225 may have an evolutionarily acquired function accompanying the appearance of the equatorial segment.

Besides its structural characteristics, the equatorial segment is well known as the egg membrane "fusion site." In fact, functional neutralization of several equatorial segment-localized proteins by antibody or gene ablation led to a reduction of the fertilizing ability of mice (Fujihara et al. 2010; Toshimori et al. 1998; Wolkowicz et al. 2008). Therefore, TMEM225 is expected to be a regulator of membrane fusion. However, membrane fusion initiates between the plasma membranes of sperm and egg, and our results suggest that the majority of TMEM225 is not localized to the plasma membrane (Fig. 5). Therefore, it does not seem likely that TMEM225 is a fusogenic component; however, we cannot entirely exclude the possibility that a small portion of TMEM225 localizes to the plasma membrane.

We also found that TMEM225 can bind to and inhibit PP1γ2. Deletion of the RVxF motif abolished the interaction, indicating that the RVxF motif is essential for function. The RVxF motif is found in more than 100 PP1 regulatory proteins with a consensus sequence of [RK]-X(0, 1)-[VI]-{P}-[FW] (X is any residue and

{P} is any residue but P), and the amino acid sequence of mouse TMEM225, ^{224}RRVTW^{228}, completely matches the consensus sequence. Many reports indicate that regulation of serine/threonine phosphorylation plays an important role in the motility and capacitation of mammalian spermatozoa. Inhibition of PP1 activity increased motility in immotile bovine caput epididymal spermatozoa (Vijayaraghavan et al. 1996) and in human ejaculated spermatozoa (Smith et al. 1996). During capacitation, adenylate cyclase is activated, and the intracellular cAMP concentration is increased, which leads to activation of protein kinase A (PKA). PKA then phosphorylates serine/threonine residues on its substrates, and the signaling cascade induces protein tyrosine phosphorylation (Visconti et al. 1995a; Visconti et al. 1995b). Accordingly, it has been reported that capacitation is accelerated by okadaic acid treatment in mouse sperm (Furuya et al. 1992). Therefore, TMEM225 is a possible regulator of motility and capacitation; however, since TMEM225 is localized to the equatorial segment and not to the midpiece and tail, involvement in motility may be excluded. Interestingly, as is often the case with somatic cells, PP1 inhibitors are activated by PKA. For instance, protein phosphatase inhibitor-1 (I-1) is inactive when not phosphorylated but becomes active once phosphorylated by PKA (Huang and Glinsmann 1976). This feedback mechanism amplifies PKA-triggered intracellular signaling. Although it is not known whether TMEM225 is activated by PKA, putative PKA phosphorylation sites were found in mouse TMEM225 by a search in NetPhosK 1.0 Server (http://www.cbs.dtu.dk/services/NetPhosK/).

In addition to sperm motility and capacitation, PP1γ2 activity is closely associated with sperm differentiation. *Ppp1cc*-deficient male mice are infertile due to impaired spermatogenesis (Varmuza et al. 1999), and *Ppp1cc*-null spermatids showed malformed heads, mitochondrial sheaths, and extra outer dense fibers (Chakrabarti et al. 2007; Forgione et al. 2010). Similarly, overexpression of Spz1 in mice, which is a helix-loop-helix type transcription factor and a putative PP1 inhibitor (Hrabchak and Varmuza 2004), induced apoptosis in male germ cells and reduced fertility (Hsu et al. 2004). These results suggest that PP1 activity and its regulation play a pivotal role in normal spermatogenesis. Remarkably, a recent study revealed that *TMEM225* expression was up-regulated ~30-fold in nonobstructive azoospemia using microarray analysis on biopsy samples (Malcher et al. 2013), suggesting that irregular expression of TMEM225 is one cause of male infertility and that TMEM225 is a potential target for diagnosis of or therapeutics for male infertility. Although further experiments using genetic targeting or animal models are necessary to elucidate its physiological function, TMEM225 may be involved with spermatogenesis through the regulation of PP1γ2.

Protein phosphorylation/dephosphorylation is critical for various cellular processes. In the human genome, over 400 serine/threonine protein kinases have been identified, but there are no more than 40

serine/threonine phosphatases (Bollen et al. 2010; Cohen 2002). This imbalance was explained by a difference in strategies for the acquisition of functional diversity. Namely, protein kinases have mainly diversified by gene duplication and subsequent specification, whereas protein phosphatases have diversified by increasing the number of regulatory proteins, which enables the spatial and temporal regulation of phosphatase activity (Cohen 2002; Hendrickx et al. 2009). In this regard, it was shown that sds22, a homolog of the yeast protein phosphatase binding protein, forms an inhibitory complex with PP1γ2 in bovine spermatozoa (Huang et al. 2002). However, whereas PP1γ2 was localized throughout spermatozoa with strong intensity in the posterior region and equatorial segment, sds22 was not present in the posterior region or equatorial segment. In addition, several PP1γ2 regulatory proteins have been found with different expression patterns in the testis (Hrabchak et al. 2007; Hrabchak et al. 2004; Huang et al. 2004). These results suggest that many proteins that are expressed in spatial and temporal-specific manners in male germ cells control the activity and substrate specificity of PP1γ2, and TMEM225 may function as one such regulator.

Materials and Methods

Animals

Mice (ICR and *W/W*^{v}) were purchased from Japan SLC (Hamamatsu, Japan). All animal experiments were approved by the Institutional Animal Care and Use Committee of Shizuoka University (permission number 26-16).

RT-PCR

Total RNA was isolated from mouse tissues with ISOGEN (Nippongene). Total RNA (5 μg) was used as a template, and reverse transcription reactions were performed with ReverTra Ace reverse transcriptase (TOYOBO) according to the manufacturer's instructions. PCR was carried out under the following conditions: 94 °C for 2 min; 30 cycles of 94 °C for 30 s, 59 °C for 30 s, and 72 °C for 60 s; and a final extension of 72 °C for 7 min. The following primer pairs were used for the expression analysis: *Tmem225*, 5′-TACTCACAGTCCATGGCTGG-3′ and 5′-CACAGAGTGCACATGGACGA-3′; *Gapdh*, 5′-CATCACCATCTTCCAGGAGCG-3′ and 5′-AAGGCCATGCCAGTGAGCTTC-3′. These primer pairs were designed to span introns to prevent the amplification of genomic DNA. PCR products were analyzed by electrophoresis on a 1.5% agarose gel, and signals were visualized by staining with ethidium bromide.

Antibodies

Two rabbit polyclonal anti-TMEM225 antibodies (#63 and #64) were raised against a KLH-conjugated peptide corresponding to the C-terminal region of mouse TMEM225 (^{217}NRPHTQARRVTWAL^{230}). Peptide synthesis, animal immunization, and sera collections were performed by Genscript. The antibodies were purified by affinity chromatography using an antigen peptide-conjugated column. Anti-FLAG monoclonal antibody (M2) and anti-Sp56 antibody (7C5) were purchased from Sigma and QED Bioscience Inc., respectively. Anti-PP1 antibody (E-9) and horseradish peroxidase-conjugated secondary antibodies were purchased from Santa Cruz Biotechnology.

Construction of expression vectors

Full-length *Tmem225* and its C-terminal region (wild-type, S162-L230; RVxF deletion mutant, S162-A223) were amplified by PCR using mouse testis cDNA as template. Mouse PP1γ2 isoform cDNA was also prepared by PCR amplification. The forward and reverse PCR primers follow: full-length *Tmem225*, 5′-AAGCTTACAATGATGCACATCCCAAAC-3′ and 5′-GGATCCGACAGAGCCCAGGTTACCCGAC-3′; *Tmem225* wild-type C-terminal region, 5′-GGATCCAGCACAAATAGATGCGAATG-3′ and 5′-AAGCTTCAGAGCCCAGGTTACCCGAC-3′; *Tmem225* RVxF deletion mutant C-terminal region, 5′-GGATCCAGCACAAATAGATGCGAATG-3′ and 5′-AAGCTTTCATGCTTGGGTGTGTGGTCTA-3′; and PP1γ2, 5′-GAATTCAATGGCGGATATCGACAAACTC-3′ and 5′-GGATCCTCACTCGTATAGGACAGTGTT-3′. Full-length *Tmem225* cDNA was cloned into pFLAG-N1, a vector modified from pEGFP-N1 (Clontech), replacing GFP with the FLAG tag sequence, and the C-terminal regions of *Tmem225* were cloned into pColdI (TaKaRa) and GST-pColdI, a vector modified from pColdI (TaKaRa) by inserting the sequence of glutathione S-transferase into the *Sac*I site. PP1γ2 cDNA was cloned into pFLAG-CMV2 (Sigma) and GST-pColdI. All sequences were confirmed by sequence analysis. All experimental procedures using recombinant DNA were approved by the Recombinant DNA Safety Committee of Shizuoka University.

Expression and purification of recombinant proteins

Escherichia coli were transformed with expression vectors constructed as above and cultured at 37 °C. Once the OD600 reached 0.6, protein expression was induced by addition of isopropyl β-D-1-thiogalactopyranoside (IPTG; final 0.2 mM) and cold shock at 15 °C. After culturing for 8–24 h, cells

were harvested. GST-tagged or 6x His-tagged recombinant proteins were purified with glutathione-sepharose beads or Ni^{2+}-NTA agarose beads, respectively, according to manufacturer's instruction. The protein solutions were dialyzed against appropriate buffers. The concentration and purity of the proteins were confirmed by sodium dodecyl sulfate-polyacrylamide gel electrophoresis (SDS-PAGE) followed by Coomassie Brilliant Blue (CBB) staining.

Cell culture, transfection, and preparation of lysate

293F cells (Invitrogen) were cultured in Dulbecco's modified Eagle's medium (Sigma D5796) supplemented with 10% fetal bovine serum and antibiotic antimycotic solution (Sigma A5955). Cells were transfected with plasmid DNAs using Polyethylenimine "Max" (Polysciences) as described previously (Boussif et al. 1995). Cultured cells were lysed with buffer containing 50 mM Tris-Cl (pH 7.4), 150 mM NaCl, 2 mM EDTA, 2 mM phenylmethylsulfonyl fluoride (PMSF), 2 mM Na_3VO_4, 20 mM NaF, and 1% Triton X-100. The lysates were separated by centrifugation for 20 min. Mouse tissues lysates were also obtained similarly.

Pull down assay, immunoprecipitation, SDS-PAGE, and western blotting

For the pull-down assay, cleared 293F lysate-expressed FLAG-tagged PP1γ2, purified GST-fusion protein (5 μg), and glutathione-sepharose beads were mixed and incubated for 12–16 h at 4 °C with gentle agitation. After washing the beads several times with lysis buffer containing 1% Trion X-100, the beads were suspended with sample buffer. For immunoprecipitation, the cell lysates or tissue lysates (500 μg of total protein) were incubated with anti-TMEM225 #63 (2 μg) at 4 °C for 12–16 h and then with protein A-sepharose beads for 2 h with gentle agitation. The immunoprecipitates were washed with lysis buffer and suspended in sample buffer. The proteins were separated by SDS-PAGE, transferred onto a polyvinylidene difluoride membrane, and detected by western blotting. To detect the signal of immunoprecipitated TMEM225, Clean-Blot IP Detection Reagent (PIERCE) was used as a secondary antibody to avoid masking by immunoglobulin light chain bands.

Sperm collection, capacitation, and acrosome reaction

Mouse epididymides were isolated and transferred into 400 μl drops of TYH medium (a modified Krebs Ringer bicarbonate solution) supplemented with 4 mg/ml bovine serum albumin (BSA) covered with mineral oil. Spermatozoa were released into the medium by cutting with scissors and pushing gently. After

removing the tissue, spermatozoa were capacitated by incubation in the medium for 1.5 h at 37 °C in a CO_2 incubator. The acrosome reaction was induced by treatment with the calcium ionophore A23187 (5 μM) or progesterone (100 μM) for 30 min. Spermatozoa were washed with PBS, smeared on poly-L-lysine-coated glass slides, air dried, and fixed with ice-cold methanol. The glass slides were stored at −30 °C until use.

Proteinase K sensitivity assay

Isolated mouse epididymal spermatozoa were washed and resuspended in PBS. A portion of the spermatozoa was centrifuged and resuspended in 1% Triton X-100 lysis buffer without PMSF. The cell suspension and cell lysate (both from an equal amount of spermatozoa) were incubated for 30 min at 37 °C in the presence or absence of proteinase K (1 μg/ml) and PMSF (1 mM). Finally, the integrity of TMEM225 was monitored by immunoprecipitation and western blotting.

Immunohistochemistry

Testes and epididymides from ICR mice were collected, fixed in Bouin's solution, embedded in paraffin, and cut into 4 μm-thick sections. The sections were mounted on poly-L-lysine-coated glass slides, deparaffinized, and rehydrated. The antigen was retrieved by heating in 1 mM EDTA (pH 8.0) using a pressure cooker for 5 min. These sections or smeared sperm samples were then blocked for 1 h with 5% skim milk in phosphate buffered saline (PBS), followed by incubation with primary antibody for 1.5 h. After washing with PBS, the samples were incubated with Alexa Fluor 488- or Alexa Fluor 568-conjugated secondary antibodies (Molecular Probes). Antibody dilutions were as follows: rabbit anti-TMEM225 #63, 10 μg/ml; rabbit anti-TMEM225 #64, 10 μg/ml; mouse anti-sp56 antibody, 1:500; Alexa Fluor-conjugated secondary antibody, 1:500. When necessary, DAPI and Alexa 488-conjugated lectin PNA (Molecular Probes) were used to stain the nuclei and acrosomes, respectively. The images were captured with a BX50 microscope (OLYMPUS) equipped with a DP50 CCD camera (OLYMPUS). For confocal microscopic analysis, the sections were stained similarly, but Alexa Fluor 633-conjugated goat anti-rabbit IgG (Molecular Probes, 1:500) was used to detect TMEM225. The images were scanned with a Leica TCL SL confocal microscope.

Measurement of PP1 activity in vitro

Phosphatase activity *in vitro* was measured by a nonradioactive assay using malachite green, which forms a colored complex with free phosphate (Fathi et al. 2002), with slight modification. Briefly, 4 μg purified

GST-PP1γ2 fusion protein and 10 μg phosphorylase a (Sigma) were incubated in 100 μl phosphatase buffer (20 mM Tris-Cl, pH 7.5, 5 mM $MgCl_2$, 1 mM EGTA, 1 mM DTT, 0.3 mg/ml bovine serum albumin, and 5 mM caffeine) for 1 h at 37 °C in the presence or absence of 6x His-tagged TMEM225 recombinant protein. Then, 200 μl of malachite green/ammonium molybdate dye solution was added to the tubes and incubated for 15 min at room temperature. The absorbance at 650 nm was measured by spectrophotometer, and the amount of released phosphate was calculated using a standard curve created with various concentrations of K_3PO_4.

Acknowledgements

This work was supported by United Graduate School of Agricultural Science (Gifu University) Education and Research Activation Grants. The authors thank Dr. Kiyotaka Toshimori and Dr. Chizuru Ito at Chiba University for their helpful discussion and Mr. Jun-ya Ohno for his technical assistance. All authors declare no conflict of interest.

References

Allen MJ, Bradbury EM, Balhorn R. 1995. The natural subcellular surface structure of the bovine sperm cell. J Struct Biol 114(3):197-208.

Bedford JM, Moore HD, Franklin LE. 1979. Significance of the equatorial segment of the acrosome of the spermatozoon in eutherian mammals. Exp Cell Res 119(1):119-126.

Bellve A, Cavicchia J, Millette C, O'Brien D, Bhatnagar Y, Dym M. 1977. Spermatogenic cells of the prepuberal mouse: isolation and morphological characterization. J Cell Biol 74(1): 68-85.

Bollen M, Peti W, Ragusa MJ, Beullens M. 2010. The extended PP1 toolkit: designed to create specificity. Trends Biochem Sci 35(8):450-458.

Boussif O, Lezoualc'h F, Zanta MA, Mergny MD, Scherman D, Demeneix B, Behr JP. 1995. A versatile vector for gene and oligonucleotide transfer into cells in culture and in vivo: polyethylenimine. Proc Natl Acad Sci U S A 92(16):7297-7301.

Carlson AE, Westenbroek RE, Quill T, Ren D, Clapham DE, Hille B, Garbers DL, Babcock DF. 2003. CatSper1 required for evoked Ca2+ entry and control of flagellar function in sperm. Proc Natl Acad Sci U S A 100(25):14864-14868.

Chakrabarti R, Kline D, Lu J, Orth J, Pilder S, Vijayaraghavan S. 2007. Analysis of Ppp1cc-null mice suggests a role for PP1gamma2 in sperm morphogenesis. Biol Reprod 76(6):992-1001.

Chun YS, Shima H, Nagasaki K, Sugimura T, Nagao M. 1994. PP1 gamma 2, a testis-specific protein-serine/threonine-phosphatase type 1 catalytic subunit, is associated with a protein having high sequence homology with the 78-kDa glucose-regulated protein, a member of the 70-kDa heat shock protein family. Proc Natl Acad Sci U S A 91(8):3319-3323.

Clermont Y. 1972. Kinetics of spermatogenesis in mammals: seminiferous epithelium cycle and spermatogonial renewal. Physiol Rev 52(1):198-236.

Cohen N, Wassarman PM. 2001. Association of egg zona pellucida glycoprotein mZP3 with sperm protein sp56 during fertilization in mice. Int J Dev Biol 45(3):569-576.

Cohen P, Cohen PT. 1989. Protein phosphatases come of age. J Biol Chem 264(36):21435-21438.

Cohen PT. 2002. Protein phosphatase 1--targeted in many directions. J Cell Sci 115(Pt 2):241-256.

Cooper MA. 2002. Optical biosensors in drug discovery. Nat Rev Drug Discov 1(7):515-528.

Eddy EM. 1998. Regulation of gene expression during spermatogenesis. Semin Cell Dev Biol 9(4):451-457.

Ellis DJ, Shadan S, James PS, Henderson RM, Edwardson JM, Hutchings A, Jones R. 2002. Post-testicular development of a novel membrane substructure within the equatorial segment of ram, bull, boar, and goat spermatozoa as viewed by atomic force microscopy. J Struct Biol 138(3):187-198.

Fathi AR, Krautheim A, Lucke S, Becker K, Juergen Steinfelder H. 2002. Nonradioactive technique to measure protein phosphatase 2A-like activity and its inhibition by drugs in cell extracts. Anal Biochem 310(2):208-214.

Forgione N, Vogl AW, Varmuza S. 2010. Loss of protein phosphatase 1c{gamma} (PPP1CC) leads to impaired spermatogenesis associated with defects in chromatin condensation and acrosome development: an ultrastructural analysis. Reproduction 139(6):1021-1029.

Fujihara Y, Murakami M, Inoue N, Satouh Y, Kaseda K, Ikawa M, Okabe M. 2010. Sperm equatorial segment protein 1, SPESP1, is required for fully fertile sperm in mouse. J Cell Sci 123(Pt 9):1531-1536.

Furuya S, Endo Y, Oba M, Nozawa S, Suzuki S. 1992. Effects of modulators of protein kinases and phosphatases on mouse sperm capacitation. J Assist Reprod Genet 9(4):391-399.

Hao Z, Wolkowicz MJ, Shetty J, Klotz K, Bolling L, Sen B, Westbrook VA, Coonrod S, Flickinger CJ, Herr JC. 2002. SAMP32, a testis-specific, isoantigenic sperm acrosomal membrane-associated protein. Biol Reprod 66(3):735-744.

Hendrickx A, Beullens M, Ceulemans H, Den Abt T, Van Eynde A, Nicolaescu E, Lesage B, Bollen M. 2009. Docking motif-guided mapping of the interactome of protein phosphatase-1. Chem Biol 16(4):365-371.

Hrabchak C, Henderson H, Varmuza S. 2007. A testis specific isoform of endophilin B1, endophilin B1t, interacts specifically with protein phosphatase-1c gamma2 in mouse testis and is abnormally expressed in PP1c gamma null mice. Biochemistry 46(15):4635-4644.

Hrabchak C, Varmuza S. 2004. Identification of the spermatogenic zip protein Spz1 as a putative protein phosphatase-1 (PP1) regulatory protein that specifically binds the PP1cgamma2 splice variant in mouse testis. J Biol Chem 279(35):37079-37086.

Hrabchak C, Varmuza S, Hrabchak C, Varmuza S. 2004. Identification of the Spermatogenic Zip Protein Spz1 as a Putative Protein Phosphatase-1 (PP1) Regulatory Protein That Specifically Binds the PP1cγ2 Splice Variant in Mouse Testis. Journal of Biological Chemistry 279(35):37079-37086.

Hsu SH, Hsieh-Li HM, Li H. 2004. Dysfunctional spermatogenesis in transgenic mice overexpressing bHLH-Zip transcription factor, Spz1. Exp Cell Res 294(1):185-198.

Huang FL, Glinsmann WH. 1976. Separation and characterization of two phosphorylase phosphatase inhibitors from rabbit skeletal muscle. Eur J Biochem 70(2):419-426.

Huang Z, Khatra B, Bollen M, Carr DW, Vijayaraghavan S. 2002. Sperm PP1γ2 Is Regulated by a Homologue of the Yeast Protein Phosphatase Binding Protein sds221.

Huang Z, Myers K, Khatra B, Vijayaraghavan S. 2004. Protein 14-3-3zeta binds to protein phosphatase PP1gamma2 in bovine epididymal spermatozoa. Biol Reprod 71(1):177-184.

Inoue N, Ikawa M, Isotani A, Okabe M. 2005. The immunoglobulin superfamily protein Izumo is required for sperm to fuse with eggs. Nature 434(7030):234-238.

Jones R, James PS, Oxley D, Coadwell J, Suzuki-Toyota F, Howes EA. 2008. The equatorial subsegment in mammalian spermatozoa is enriched in tyrosine phosphorylated proteins. Biol Reprod 79(3):421-431.

Kim KS, Cha MC, Gerton GL. 2001. Mouse sperm protein sp56 is a component of the acrosomal matrix. Biol Reprod 64(1):36-43.

Malcher A, Rozwadowska N, Stokowy T, Kolanowski T, Jedrzejczak P, Zietkowiak W, Kurpisz M. 2013. Potential biomarkers of nonobstructive azoospermia identified in microarray gene expression analysis. Fertil Steril 100(6):1686-1694.e1681-1687.

Phillips DM. 1977. Surface of the equatorial segment of the mammalian acrosome. Biol Reprod 16(1):128-137.

Schultz N, Hamra FK, Garbers DL. 2003. A multitude of genes expressed solely in meiotic or postmeiotic spermatogenic cells offers a myriad of contraceptive targets. Proc Natl Acad Sci U S A 100(21):12201-12206.

Shima JE, McLean DJ, McCarrey JR, Griswold MD. 2004. The murine testicular transcriptome: characterizing gene expression in the testis during the progression of spermatogenesis. Biol Reprod 71(1):319-330.

Smith GD, Wolf DP, Trautman KC, da Cruz e Silva EF, Greengard P, Vijayaraghavan S. 1996. Primate sperm contain protein phosphatase 1, a biochemical mediator of motility. Biol Reprod 54(3):719-727.

Toshimori K, Saxena DK, Tanii I, Yoshinaga K. 1998. An MN9 antigenic molecule, equatorin, is required for successful sperm-oocyte fusion in mice. Biol Reprod 59(1):22-29.

Varmuza S, Jurisicova A, Okano K, Hudson J, Boekelheide K, Shipp EB. 1999. Spermiogenesis is impaired in mice bearing a targeted mutation in the protein phosphatase 1cgamma gene. Dev Biol 205(1):98-110.

Vijayaraghavan S, Stephens DT, Trautman K, Smith GD, Khatra B, da Cruz e Silva EF, Greengard P. 1996. Sperm motility development in the epididymis is associated with decreased glycogen synthase kinase-3 and protein phosphatase 1 activity. Biol Reprod 54(3):709-718.

Visconti PE, Bailey JL, Moore GD, Pan D, Olds-Clarke P, Kopf GS. 1995a. Capacitation of mouse spermatozoa. I. Correlation between the capacitation state and protein tyrosine phosphorylation. Development 121(4):1129-1137.

Visconti PE, Moore GD, Bailey JL, Leclerc P, Connors SA, Pan D, Olds-Clarke P, Kopf GS. 1995b. Capacitation of mouse spermatozoa. II. Protein tyrosine phosphorylation and capacitation are regulated by a cAMP-dependent pathway. Development 121(4):1139-1150.

Wolkowicz MJ, Digilio L, Klotz K, Shetty J, Flickinger CJ, Herr JC. 2008. Equatorial segment protein (ESP) is a human alloantigen involved in sperm-egg binding and fusion. J Androl 29(3):272-282.

Wolkowicz MJ, Shetty J, Westbrook A, Klotz K, Jayes F, Mandal A, Flickinger CJ, Herr JC. 2003. Equatorial segment protein defines a discrete acrosomal subcompartment persisting throughout acrosomal biogenesis. Biol Reprod 69(3):735-745.

Yang S, Wang W, Lei C, Liu Q, Xu F, Xing X, Chen H, Liu J, Wu S, Wang M. 2011. Localization and characterization of rat transmembrane protein 225 specifically expressed in testis. DNA Cell Biol 30(1):9-16.

Yogo K, Tojima H, Ohno JY, Ogawa T, Nakamura N, Hirose S, Takeya T, Kohsaka T. 2012. Identification of SAMT family proteins as substrates of MARCH11 in mouse spermatids. Histochem Cell Biol 137(1):53-65.

Figure Legends

Figure 1. Expression of *Tmem225* in mouse tissues

A) Expression of *Tmem225* in various mouse tissues was investigated using reverse transcription-polymerase chain reaction. *Gapdh* was used as an internal control. B) Expression of *Tmem225* in wild-type and W/W^v mouse testes. C) Postnatal testicular expression of *Tmem225*. The numbers indicate the days after birth.

Figure 2. TMEM225 is expressed in the testis and epididymal sperm

A) Validation of antibody specificity. FLAG-tagged TMEM225 was expressed in 293F cells and immunoprecipitated with anti-TMEM225 antibody. The precipitates were detected by western blotting using anti-TMEM225 antibody or anti-FLAG antibody. B) Expression of TMEM225 in various mouse tissues was monitored by immunoprecipitation (IP)-western blotting. C) Testicular expression of TMEM225 during postnatal development. The numbers indicate the days after birth. D) Expression of TMEM225 in male reproductive organs and cauda epididymal sperm (sperm) was monitored as in B). Cont IgG, normal rabbit IgG used as a control.

Figure 3. Immunohistochemical analysis of TMEM225 in the testis and epididymis

A) Tissue sections were stained with anti-TMEM225 antibody. The immunofluorescence signal was detected in the inner layer of some seminiferous tubules in the testis (upper panel) and lumen of epididymal duct (lower panel). Nuclei were stained with DAPI. B) Stage-dependent expression of TMEM225. TMEM225 is expressed in spermatids of the maturation phase (steps 15–16) at stages IV–VIII. Roman numerals and Arabic numerals indicate the stages of the cycle of the seminiferous epithelium and the developmental steps of spermatids, respectively. Bar, 40 μm.

Figure 4. Intracellular localization of TMEM225 in mature spermatozoa

A) Immunostaining of TMEM225 in spermatozoa. *left*: lower magnification, *right*: higher magnification. BF: bright field. Bar, 10 μm. B) Immunostaining of TMEM225 using absorbed antibody and another anti-TMEM225 antibody. C) Double immunofluorescence staining of TMEM225 (red) and sp56 (green), a marker for the anterior region of the acrosome. D) Double immunofluorescence staining of TMEM225 and peanut agglutinin (PNA) in vertical sections of cauda epididymal spermatozoa. The region between arrowheads indicates the presumed equatorial segment. Bar, 10 μm.

Figure 5. Proteinase K sensitivity of TMEM225

Intact spermatozoa or cell extracts were incubated in the presence or absence of proteinase K (1 μg/ml) and PMSF (1 mM). The integrity of TMEM225 was monitored by immunoprecipitation (IP)-western blotting.

Figure 6. Effect of capacitation and acrosome reaction on intracellular localization of TMEM225

A) Double immunostaining of non-capacitated (a-c), capacitated (d-f), and acrosome reacted (g–l) spermatozoa. The acrosome reaction was induced by a calcium ionophore (g–i) or progesterone (j–l). TMEM225 (a, d, g, j), sp56 (b, e, h, k), and merged images of TMEM225 and bright field (c, f, i, l). TMEM225 in the dorsal region of the acrosome is slightly decreased after the acrosome reaction (arrowhead). Bar, 10 μm. B) Quantification of TMEM225 staining area (pixels) in non-capacitated, capacitated, and acrosome-reacted spermatozoa with image software. Data are expressed as the mean ± standard deviation of ~100 spermatozoa from two independent experiments. Different superscripts indicate significant differences ($P < 0.05$) between groups.

Figure 7. Interaction between TMEM225 and PP1γ2

A) The interaction of TMEM225 with PP1 *in vivo* was analyzed by immunoprecipitation (IP)-western blotting using epididymal lysate. B) The pull-down assay was performed as described in Materials and Methods. Interaction of the C-terminal region of TMEM225 and FLAG-tagged PP1γ2 was observed in wild-type TMEM225 but not in the RVxF mutant. Equal volumes of recombinant proteins were confirmed by Coomassie brilliant blue (CBB) staining. C) Effect of TMEM225 on phosphatase activity *in vitro*. Data are expressed as the mean ± standard error (n = 5). Black circle: wild-type, triangle: RVxF mutant.

Figure 1

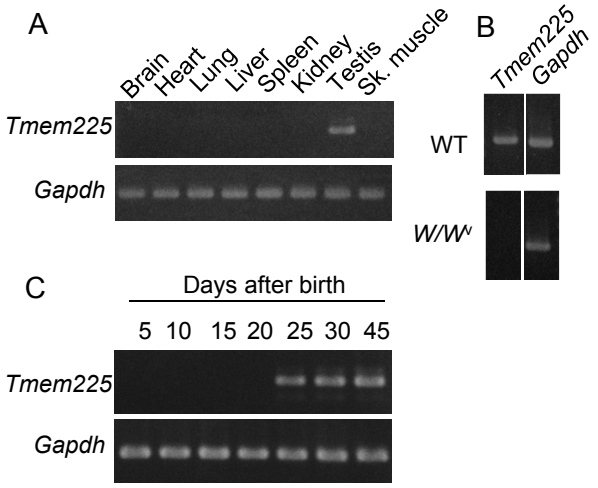
A
Brain
Heart
Lung
Liver
Spleen
Kidney
Testis
Sk. muscle
Tmem225
Gapdh
B
Tmem225
Gapdh
WT
W/Wv
C
Days after birth
5 10 15 20 25 30 45
Tmem225
Gapdh

Figure 2

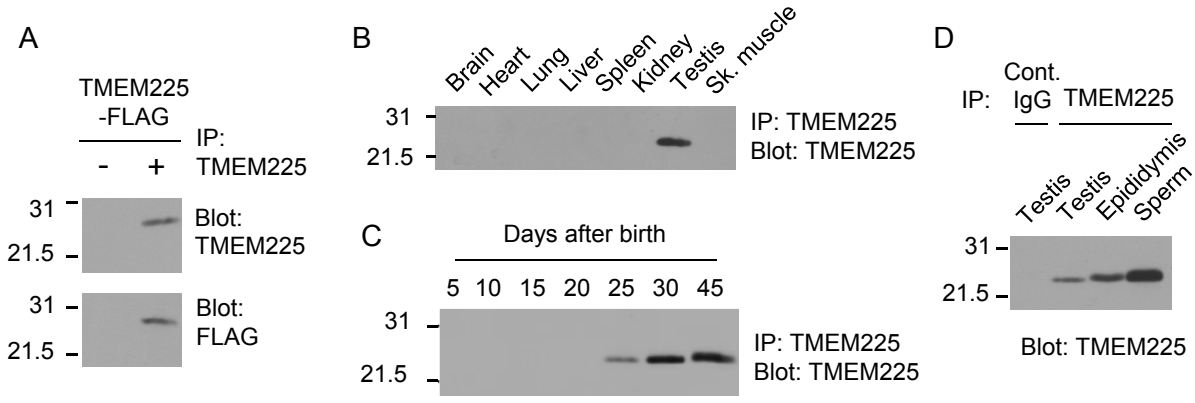
A
TMEM225
-FLAG
IP:
TMEM225
-
+
31
21.5
Blot:
TMEM225
31
21.5
Blot:
FLAG
B
Brain
Heart
Lung
Liver
Spleen
Kidney
Testis
Sk. muscle
31
21.5
IP: TMEM225
Blot: TMEM225
C
Days after birth
5 10 15 20 25 30 45
31
21.5
IP: TMEM225
Blot: TMEM225
D
Cont.
IP:
IgG
TMEM225
Testis
Testis
Epididymis
Sperm
31
21.5
Blot: TMEM225

Figure 3

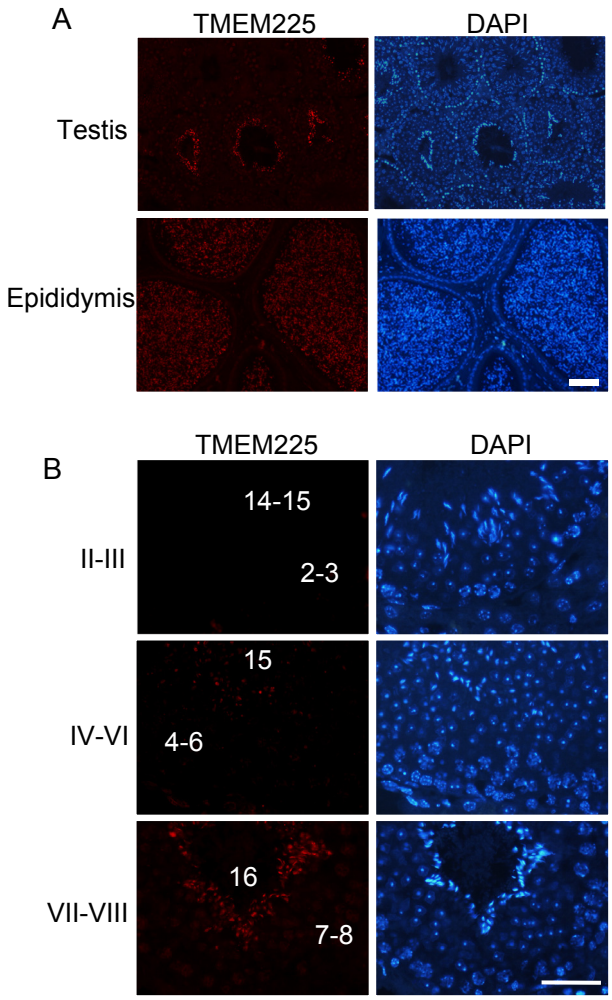
A
TMEM225
DAPI
Testis
Epididymis
B
TMEM225
DAPI
14-15
2-3
II-III
15
4-6
IV-VI
16
7-8
VII-VIII

Figure 4

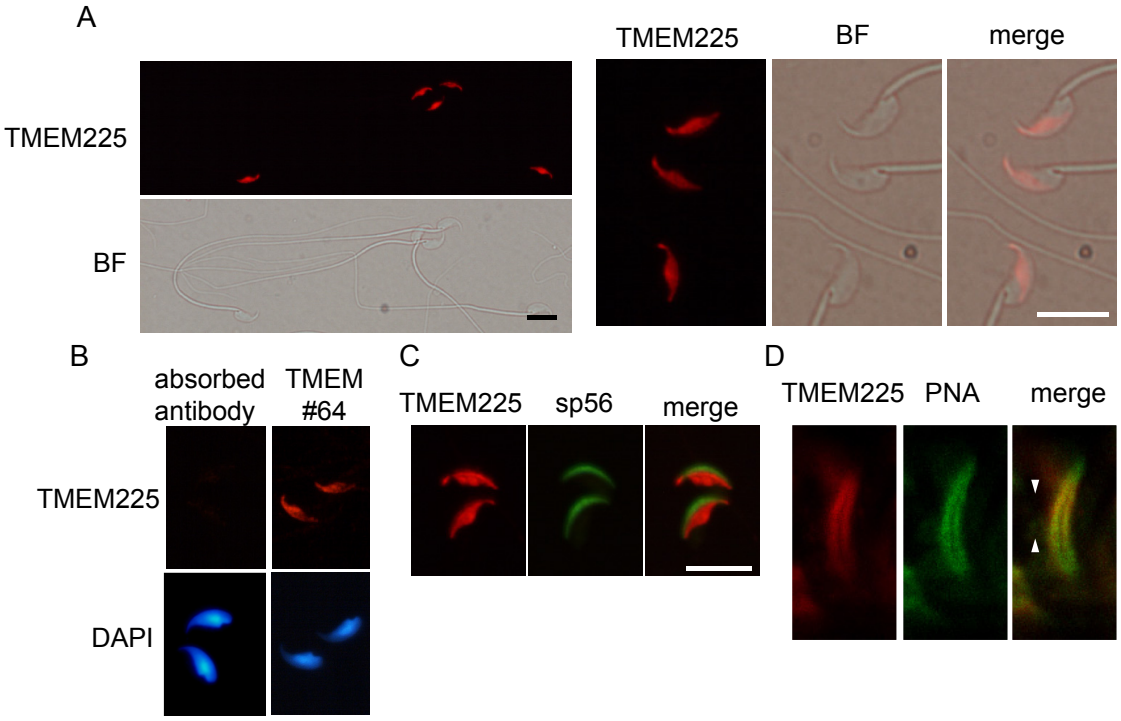
A
TMEM225
BF
TMEM225
BF
merge
B
absorbed antibody
TMEM #64
TMEM225
DAPI
C
TMEM225
sp56
merge
D
TMEM225
PNA
merge

Figure 5

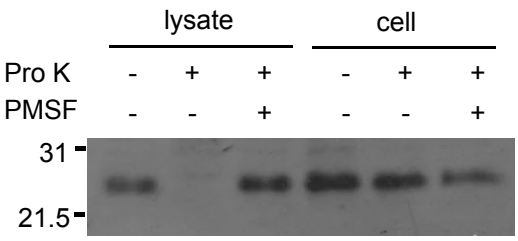

Figure 6

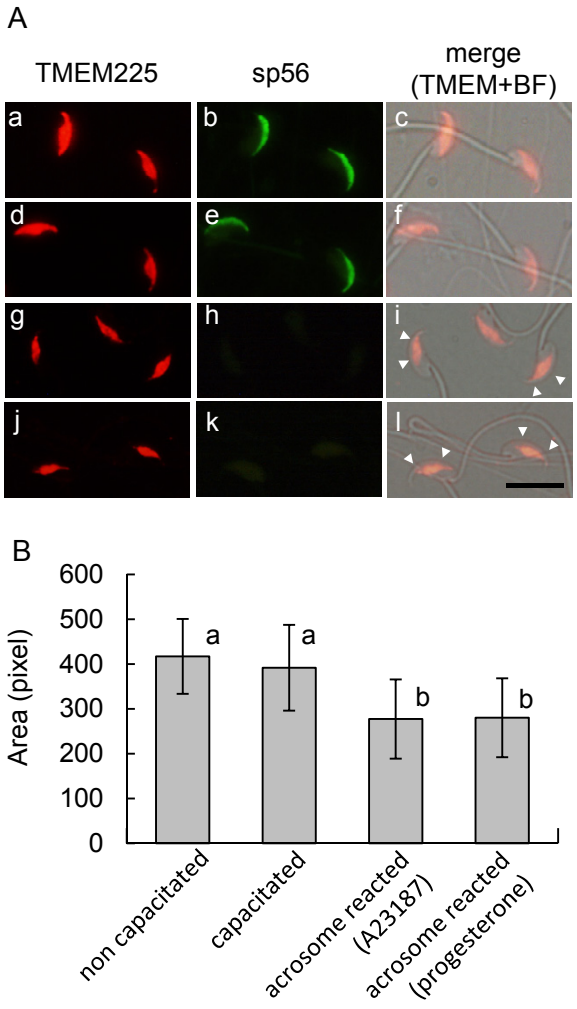
A
TMEM225
sp56
merge
(TMEM+BF)
a
b
c
d
e
f
g
h
i
j
k
l
B
Area (pixel)
600
500
400
300
200
100
0
a
a
b
b
non capacitated
capacitated
acrosome reacted
(A23187)
acrosome reacted
(progesterone)

Figure 7

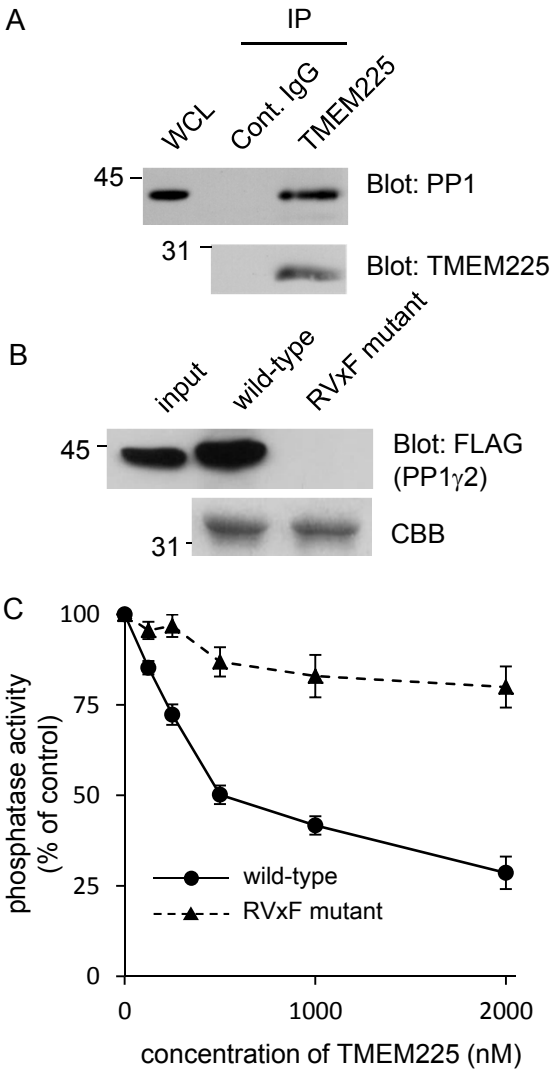
A
IP
WCL
Cont. IgG
TMEM225
45
Blot: PP1
31
Blot: TMEM225
B
input
wild-type
RVxF mutant
45
Blot: FLAG
(PP1γ2)
31
CBB
C
100
75
50
25
0
phosphatase activity
(% of control)
wild-type
RVxF mutant
0
1000
2000
concentration of TMEM225 (nM)